*Asian Journal of Environment & Ecology*

*8(4): 1-10, 2018; Article no.AJEE.47337*
*ISSN: 2456-690X*

# Wind Power Potential in Near Future Climate Scenarios: The Case for Burundi (East Africa)

**Agnidé Emmanuel Lawin[1], Manirakiza Célestin[2*] and Lamboni Batablinlé[2]**

*[1]University of Abomey-Calavi (UAC), P.O.Box 2041, Calavi, Benin.*
*[2]Institute of Mathematics and Physical Sciences, UAC, 01 P.O.Box 613, Porto-Novo, Benin.*

***Authors' contributions***

*This work was carried out in collaboration among all authors. The first author AEL designed the study and developed the methodology. Author MC performed the field work and computer analysis. Authors AEL, MC and LB contributed to results analysis and interpretation. Overall the authors contributed equally to this paper.*

***Article Information***

DOI: 10.9734/AJEE/2018/v8i430080
Editor(s):
(1) Dr. Adamczyk Bartosz, Department of Food and Environmental Sciences, University of Helsinki, Finland.
Reviewers:
(1) Hamrouni Nejib, University of carthage, Tunisia.
(2) Dr. Hardiansyah, Tanjungpura University, Indonesia.
(3) Raheel Muzzammel, University of Lahore, Pakistan.
Complete Peer review History: http://www.sdiarticle3.com/review-history/47337

***Original Research Article***

***Received 05 November 2018***
***Accepted 13 February 2019***
***Published 07 March 2019***

## ABSTRACT

This paper assessed projected changes of wind power potential in near future climate scenarios over four sites from two contrasting regions of Burundi. Observed and MERRA-2 data sets were considered for the historical period 1981-2010, and a computed Multi-model ensemble for future projections data of eight Regional Climate Models under RCP 4.5 and 8.5 over the period 2011-2040 was used. Regional Climate Models were downscaled at local climate using Empirical Statistical Downscaling method. Mann-Kendall's test was used for trend analysis over the historical period, while future changes in wind power density (WPD) quartiles were computed for each climate scenario by 2040. The findings revealed an increase in wind power potential all over the area studied with higher values during summer time. Indeed, over the period 2011-2040, the lowest WPD change is projected at Northern highlands (NHL) under RCP 4.5 with 27.03 $W.m^{-2}$, while the highest WPD change of 46.34 $W.m^{-2}$ is forecasted under RCP 8.5 at Southern Imbo plain (SIP). The month of August and September are expected to have higher WPD change in RCP 4.5 and RCP 8.5, respectively while January is projected to have the lowest WPD. Places near by the Lake Tanganyika are the most favorable areas for wind power generation.

**Corresponding author: E-mail: manirakiza_celest@yahoo.fr;*

*Keywords: Burundi; climate change; wind power.*

## ABBREVIATIONS

*MERRA-2 : Modern Era Reanalysis for Research and Applications version 2*
*MK : Mann-Kendall*
*NHL : Northern Highlands*
*NIP : Northern Imbo Plain*
*RCP : Representative Concentration Pathways*
*RCM : Regional Climate Model*
*SHL : Southern Highlands*
*SIP : Southern Imbo Plain*
*WPD : Wind Power Density*
*WS : Wind Speed*

## 1. INTRODUCTION

Climate change effects vary from one region to another depending on various socio economic and environmental factors [1]. Globally, climate change is predicted to cause stronger surface wind speed values across the boreal regions of the Northern Hemisphere, including much of Canada, Siberia and northern Europe, and in tropical and subtropical regions in Africa, and Central and South America. However, Greenland, southern Europe, China, India, southern Australia and much of the west coast of South America are expected to experience decreasing wind speed values [2]. To mitigate climate change impacts, renewable sources have received considerable attention in power generation [3]. Therefore, the increasing demand for renewable energy sources in the coming decades requires that we have a clear understanding of the susceptibility of these resources to climate change [4,5]. Burundi is an East African country heavily dependent on hydropower for his electricity production and experiences power shortage during the dry seasons [6]. To supplement the shortfall of electricity fossil fuels have become an alternative solution [7] which contributes to the environment destruction. However, Burundi has average wind speeds varying between 4 $m.s^{-1}$ and 6 $m.s^{-1}$ [8] which, if thoroughly investigated, could be used to a large extent to reduce the dependence of fossil fuels in electricity generation. Therefore, this study aims to analyze the wind power potential in near future climate. Specifically, we determine the wind power potential over the current period 1981 - 2010 and analyze the projected changes over the period 2011-2040 under climate scenarios RCP 4.5 and 8.5 by considering four sites (Northern Highlands, Northern Imbo Plain, Southern Highlands and Southern Imbo Plain) from two contrasting regions; western lowlands and highlands of Burundi.

## 2. MATERIALS AND METHODS

### 2.1 Study Area

The Fig. 1 shows the study area location in Burundi, an East African country between longitudes 28.8° and 30.9° East and latitudes 2.3° and 4.45° South [9]. Bounded to the north by Rwanda, to the East and South by Tanzania and to the West by the Democratic Republic of Congo (DRC), Burundi covers an area of 27834 $km^2$ [10]. The study area elevation is between 1800 and 2650 m altitude in the highlands while lowlands are between 774 and 1000 m altitude. The studied sites are highlands and western lowlands of Burundi. For better analysis, the highlands were divided into Northern Highlands (NHL) and Southern Highlands (SHL) while the western lowlands were split into Northern Imbo Plain (NIP) and Southern Imbo Plain (SIP).

### 2.2 Data Source

Three sets of data are used in this study. The first set consists of observed data collected from the meteorological stations of Burundi located in Fig. 1 belonging to the Geographical Institute of Burundi (IGEBU). Wind speed observed data were collected over the period 1981-2010 at hourly scales. However, only the station of Bujumbura (Airport) was able to cover the considered period 1981-2010, a period which respects the normal of 30 years at least, recommended by World Meteorology Organization (WMO). To complement observed values at hourly scales, the second set of data grouping MERRA-2 (Modern Era Reanalysis for Research and Applications Version 2) data available online at [https://gmao.gsfc.nasa.gov/reanalysis/MERRA-2/] was used. This data set is very useful in view of the fact that weather stations are limited in number, unevenly distributed, have missing data problem and short period of observation [11]. Missing observed data have been filled using cross validation method following Ioannis [12].

For future climate, the third data set groups wind speeds from eight Regional Climate Models downscaled at climate stations using Empirical Statistical Downscaling [13]. The Table 1

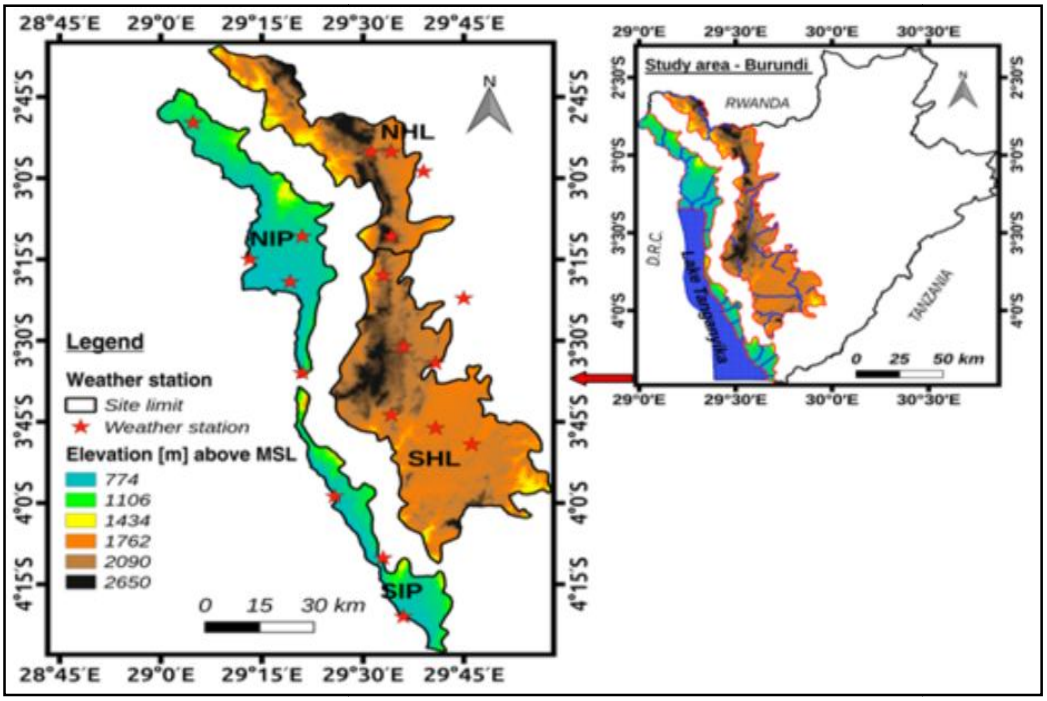


**Fig. 1. Study area location**

provides concise information on the used Models to run the Multi-Model ensemble.

This data set is available in the context of the COordinated Regional Climate Downscaling Experiment (CORDEX) over Africa at 0.44° resolution for the period 1950 to 2100 [14] and accessed online [https://www.cordex.org] through user registration. RCM historical data have been used for bias correction. Furthermore, in this study, we considered wind speeds at 12 m height, the height at which IGEBU data were collected. MERRA-2 and RCM wind speeds data were however at 10 m height and the power law [15] was used to calculate wind speeds at 12 m height. Furthermore, MERRA-2 data were compared to available ground data before it was used to complement observations and adopted as observed data in this study. The same procedure has been used by Asfaw et al. [11].

The power of the wind at 12 m height was computed following Wilkie et al. [16] while the trend analysis was done using the Mann-Kendall's (MK) test (1945) [17,18] at the threshold $\alpha = 0.05$ . Furthermore, the spatial distribution of wind power density was mapped using Inverse Distance Weighted (IDW) interpolation method [19]. Climate Data Operators [20] and R program [21] have been used for data computation, analysis and visualization. The procedural steps highlighted in Fig. 2 were used in this study.

**Table 1. Climatic models used**

| Global climate model name | Institute ID | Model short name | Model origin country |
|---|---|---|---|
| CanESM2 | CCCma | CCCma | Canada |
| CNRM-CM5 | CNRM-CERFACS | CNRM | France |
| EC-EARTH | ICHEC | ICHEC | Europe |
| IPSL-CM5A-MR | IPSL | IPSL | France |
| MIROC5 | MIROC | MIROC | Japan |
| MPI-ESM-LR | MPI-M | MPI | Germany |
| NorESM1-M | NCC | NCC | Norway |
| GFDL-ESM2M | NOAA-GFDL | NOAA | USA |

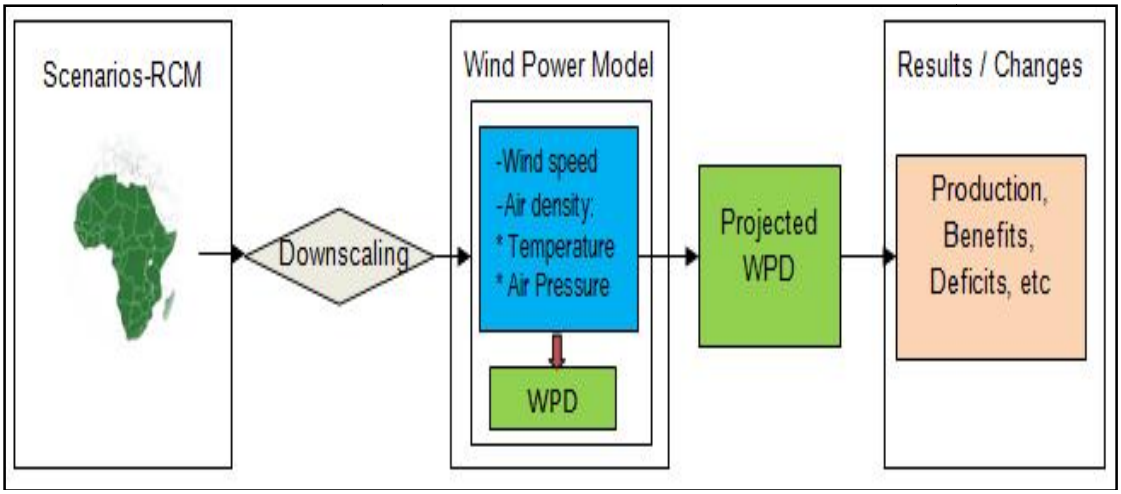


**Fig. 2. Used steps in assessing the impacts from near future climate scenarios to wind power potential**

## 3. RESULTS AND DISCUSSION

### 3.1 Monthly and Annual Wind Potential

The Fig. 3 shows the monthly wind potential over the current period 1981-2010 at NHL, NIP, SHL and SIP. The figure highlights that from May (5) to September (9), the average wind speed (WS) is greater than 4 $m.s^{-1}$ all over the four sites. This period of high WS coincides with the long dry season. Indeed, the SIP site is revealed to have the highest WS from January to December. On the other hand, the same figure presents the Air density over the four sites. The highlands sites (NHL and SHL) have lower air density than lowlands sites; which is obviously explained by the elevation between the two regions (Fig. 1). These two parameters are very important for wind power computing [16].

The Fig. 4 compares MERRA-2 (observation) and downscaled RCM wind speed at annual scale, calibrated over the period 1981-2010. The performance was objectively measured based on Nash efficiency criterion, $R^2$ for each site. In fact, $R^2$ was found equal to 0.85, 0.96, 0.92 and 0.94 at NHL, NIP, SHL and SIP, respectively. Furthermore, the similarity between MERRA-2 and downscaled RCM distribution was measured based on Kolmogorov-Smirnov test. Indeed, the distance between the two distribution function was found equal to 0.4 with a p-value of 0.69, 0.2 with a p-value of 0.96, 0.14 with a p-value of 0.97 and 0.33 with a p-value of 0.97 at NHL, NIP, SHL and SIP, respectively. Statistically, the two distribution function are the same at significance level $\alpha = 0.05$.

### 3.2 Monthly and Annual Wind Power Potential

The Fig. 5 presents the monthly distribution of wind power density (WPD) over the reference period 1981-2010.

The figure highlights areas in low and high WPD for the twelve months of the year. Therefore, from June to September, we have months in high WPD with values greater than 60 $W.m^{-2}$ while from November to March, we have months in low WPD with values less than 25 $W.m^{-2}$. The findings show that the months of April, May and October have WPD between 25 and 60 $W.m^{-2}$. Furthermore, within the four sites, SIP is revealed to have higher WPD than other sites over the entire baseline period with values greater than 120 $W.m^{-2}$ during the summer time. Moreover, MK's test detected an upward trend in WPD at significance level equals to 0.05. The Kendall's tau of 0.31, 0.38, 0.36 and 0.49 with their respective p-values equal to 0.0098, 0.0016, 0.0033 and < 0.0001 were revealed at NHL, NIP, SHL and SIP, respectively. However, from the results, the four sites are only promising for installing wind turbine for small-scale power generation. In addition, the demand of water for irrigation is seasonal and it is found that the highest wind power density coincides with the dry season which may favor wind powered water pumping applications. Otherwise, large-scale wind power generates at least 200 $W.m^{-2}$ which

require that mean wind speeds exceed 7 m/s [15].

### 3.3 Future Wind Power Potential

The Fig. 6 and Fig. 7 present the spatial projected monthly WS following RCP 4.5 and RCP 8.5, respectively. The analysis of the Fig. 3 shows that, from October to March, projected WPD is below 60 W.m$^{-2}$ all over the study area. The months June-September are forecasted to have the highest WPD above 120 W.m$^{-2}$. Among the four sites, SIP is expected to experience the highest WPD. Furthermore, the south of NIP will experience higher WPD than other parts of NIP. Moreover, the southern parts of SHL are projected to be in higher WPD than other parts of SHL. Likewise, the analysis of the Fig. 4 reveals that, from October to April, the WPD is projected to be below 100 W.m$^{-2}$ while the months May-September are forecasted to experience WPD above 120 W.m$^{-2}$. Higher WPD is projected at SIP with values greater than 250 W.m$^{-2}$ in September. Comparing findings from RCP 4.5 with RCP 8.5, WPD values are higher in RCP 8.5 with a slight difference except at SIP in September.

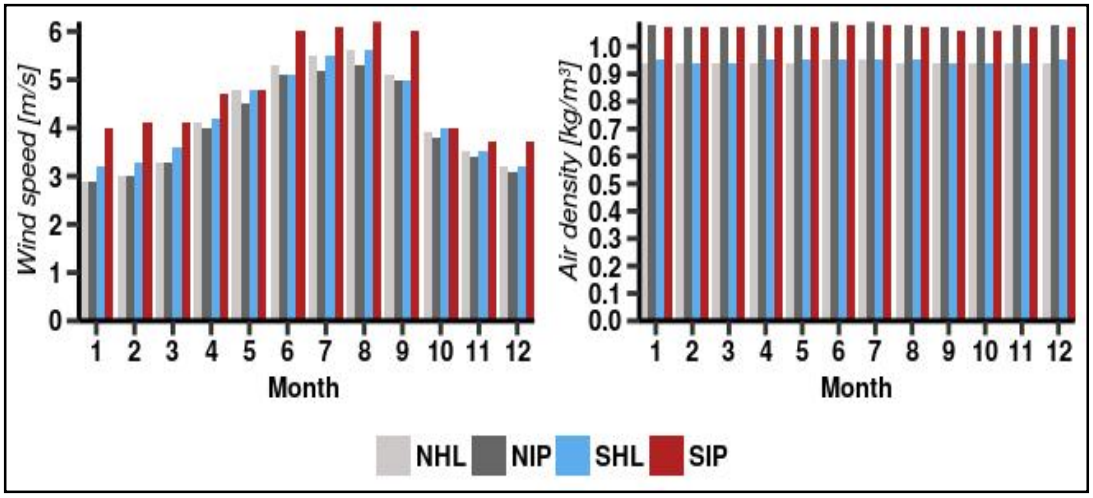


**Fig. 3. Monthly wind potential and air density over the period 1981 – 2010**

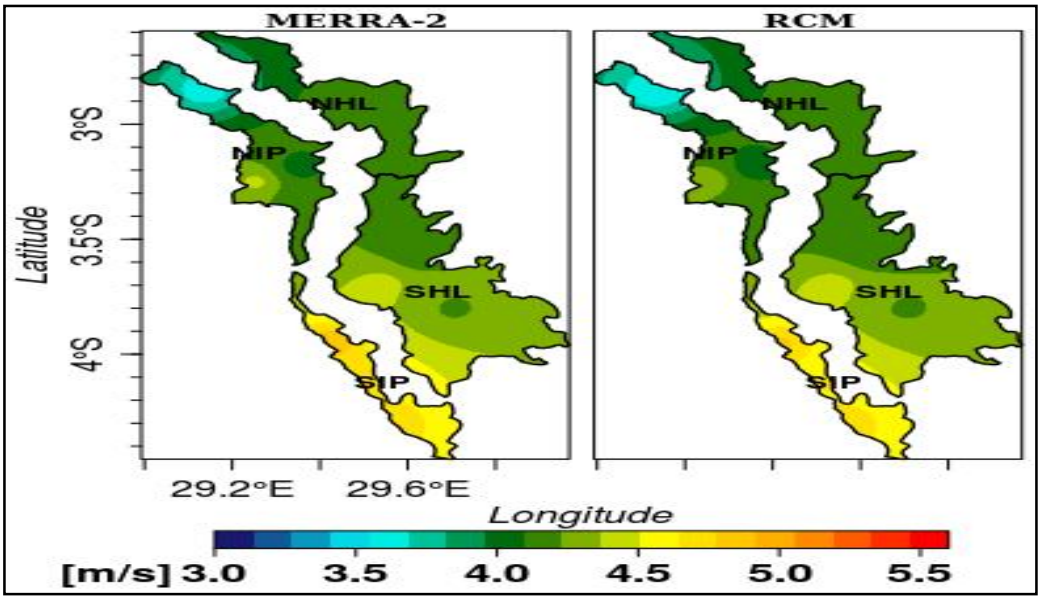


**Fig. 4. MERRA-2 and downscaled RCM wind speed over the period 1981 - 2010**

### 3.4 Wind Power Density Projected Changes

The Fig. 8 uses violins to explain WPD projected changes. The red dot shows the mean of projected WPD changes. The thicker part indicates that the monthly WPD change value in that section of the violin has higher frequency, and the thinner part implies lower frequency. The bottom of the violin shows the minimum WPD change value while the top of the violin means the maximum value. For more clarity, only months corresponding to the maximum and minimum changes have been visualized with the violin. Furthermore, the first crossbar of the violin marks the 1st quartile, the second crossbar is the 2nd quartile (median) and the last is the 3rd quartile.

Therefore, in RCP 4.5, an average WPD change of 27.03 W.m$^{-2}$, 29.28 W.m$^{-2}$, 27.14 W.m$^{-2}$ and 30.08 W.m$^{-2}$ is projected at NHL, NIP, SHL and SIP, respectively by 2040. Although these changes are close, the analysis shows that WPD changes in lowlands (NIP and SIP) are higher than highlands (NHL and SHL). All over the four sites, the month of August is projected to experience the highest WPD changes while January will have the lowest. In August the highest WPD change value is expected at SIP with 49.7 W.m$^{-2}$, while in January the lowest change will be at NHL with 11.6 W.m$^{-2}$. Likewise, following RCP 8.5, the month of September is expected to have the highest WPD changes all over the study area. Indeed, in the lowlands, September shows the higher changes than highlands where SIP is expected to experience the highest WPD change value equal to 98.6 W.m$^{-2}$. Overall, in RCP 8.5, NHL, NIP, SHL and SIP are projected to experience WPD changes equal to 27.2 W.m$^{-2}$, 30.21 W.m$^{-2}$, 27.44 W.m$^{-2}$ and 46.34 W.m$^{-2}$, respectively. Both the scenarios agree on January as a projected month to experience the lowest WPD changes across the lowlands and highlands.

### 3.5 Annual Spatial Distribution of Projected WPD Changes

The Fig. 9 presents the spatial distribution of annual WPD changes over the period 2011-2040 (11/40) following RCP 4.5 and RCP 8.5 according to the reference period 1981-2010. The figure shows that changes are expected to be higher in RCP 8.5 than RCP 4.5. In fact, changes in RCP 4.5 will be less than 30 W.m$^{-2}$ while changes in RCP 8.5 will be higher than 25 W.m$^{-2}$.

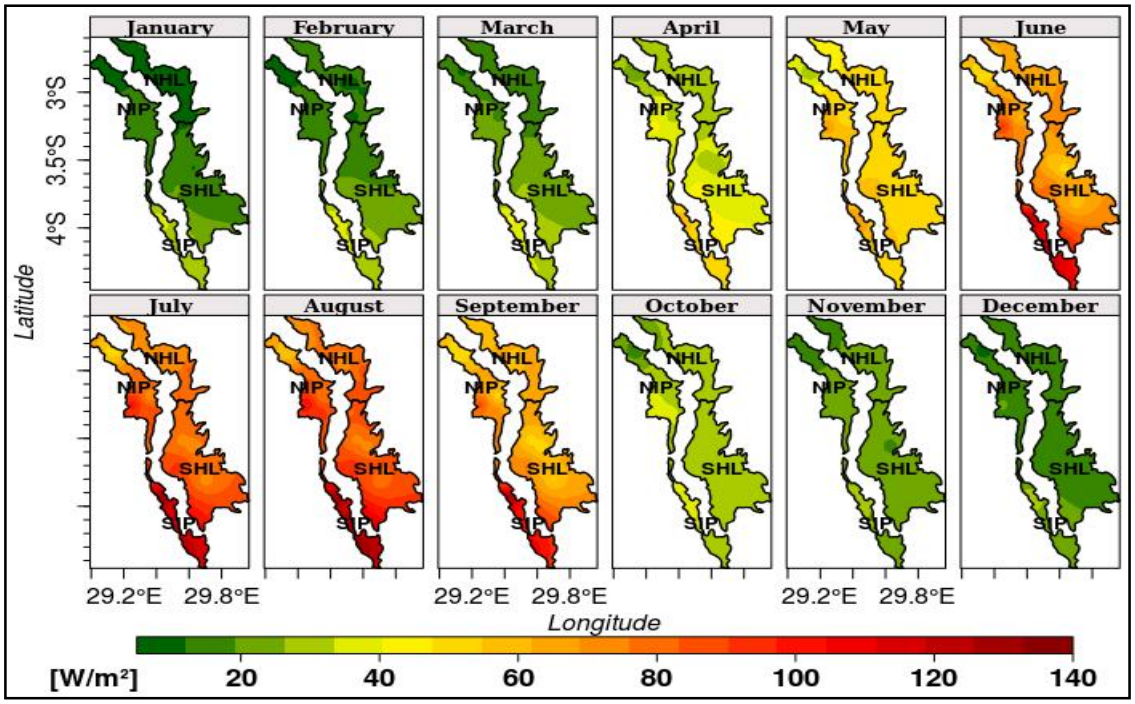


**Fig. 5. Monthly and annual wind power potential over the period 1981 - 2010**

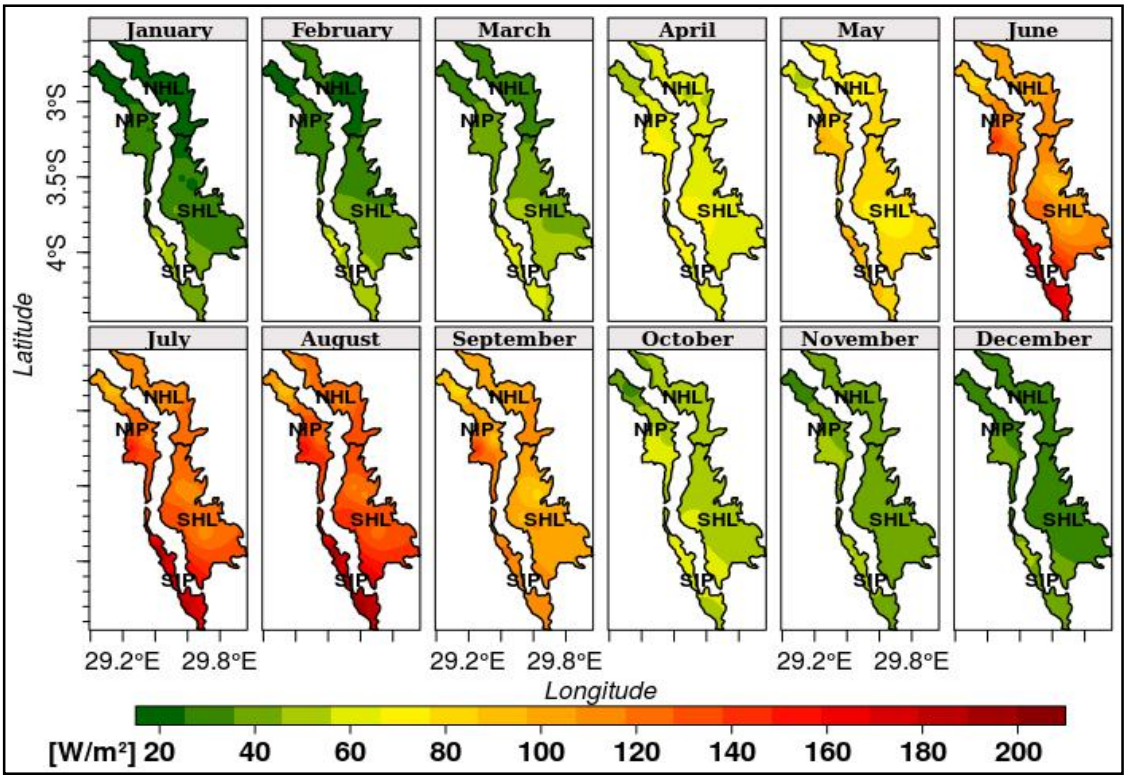


**Fig. 6. Monthly and annual WPD over the period 2011 – 2040 under RCP 4.5**

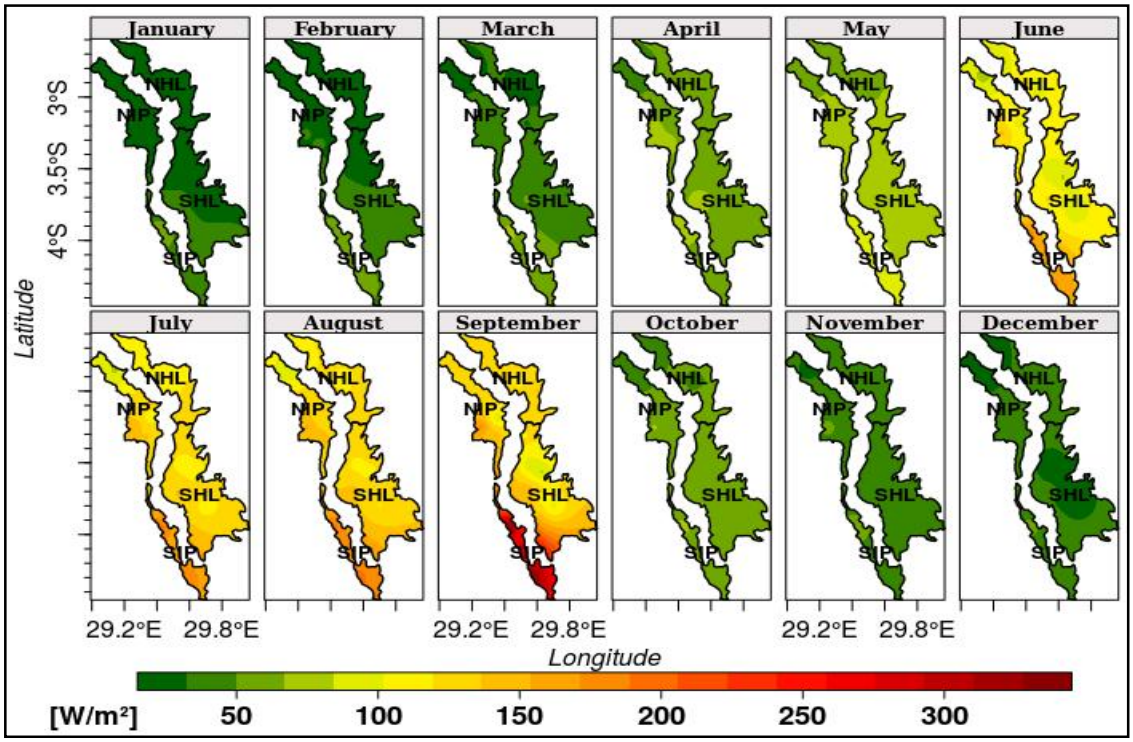


**Fig. 7. Monthly and annual WPD over the period 2011 – 2040 under RCP 8.5**

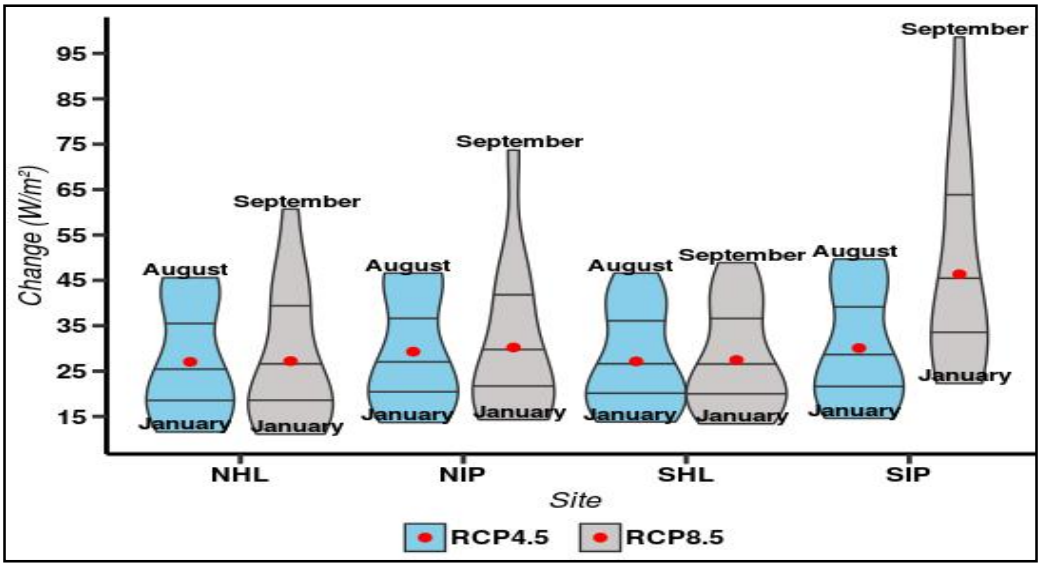


**Fig. 8. Projected monthly and annual average WPD changes over the period 2011-2040 under RCP 4.5 and RCP 8.5**

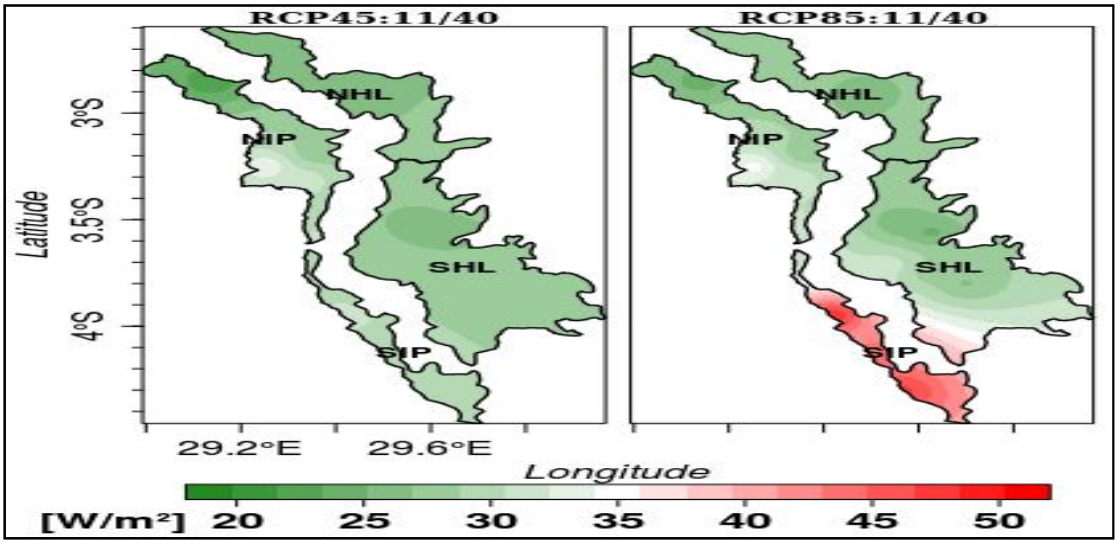


**Fig. 9. Spatial distribution of annual WPD change by 2040 under RCP 4.5 and RCP 8.5**

Furthermore, western areas near by the Lake Tanganyika are expected to experience higher increase in WPD than other areas. Indeed, the entire SIP is projected to experience sensitive changes in RCP 8.5.

The findings from this study projecting increase in WPD are consistent with many studies projecting increase in wind speeds from different regions of the globe as well as studies from East Africa [1,22-25] as the result of the global climate change.

## 4. CONCLUSION

Future Climate Scenarios showed that wind power potential is expected to increase in the highlands and western lowlands of Burundi over the period 2011 – 2040.

In the future climate, following RCP 4.5, an average WPD change of 27.03 $W.m^{-2}$, 29.28 $W.m^{-2}$, 27.14 $W.m^{-2}$ and 30.08 $W.m^{-2}$ is projected at NHL, NIP, SHL and SIP, respectively. All over the four sites, the month of August is projected to

experience the highest WPD change. On the other hand, following RCP 8.5, the month of September is expected to have the highest WPD change all over the study area. The sites NHL, NIP, SHL and SIP are projected to experience WPD changes equal to 27.2 $W.m^{-2}$, 30.21 $W.m^{-2}$, 27.44 $W.m^{-2}$ and 46.34 $W.m^{-2}$, respectively in RCP 8.5. Both the scenarios agree on January as a projected month to experience the lowest WPD changes across the western lowlands and highlands of Burundi. Furthermore, both climate scenarios agree on SIP as the site expected to experience the highest WPD by 2040. The findings highlighted that areas near by the Lake Tanganyika are expected to experience higher increase in WPD than other areas.

## COMPETING INTERESTS

Authors have declared that no competing interests exist.

## REFERENCES


1. IPCC. Towards new scenarios for analysis of emissions, climate change, impacts and response strategies. Noordwijkerhout, The Netherlands; 2007.
2. Scott E, James M, Bart N, Wood A. Climate change effects on wind speed. NAm Wind. 2008;7:68-72.
3. Hasan MM, Wyseure G. Impact of climate change on hydropower generation in Rio Jubones Basin, Ecuador. Water Science and Engineering. 2018;11(2):157-166.
4. Davy R, Gnatiuk N, Pettersson L, Bobylev L. Climate change impacts on wind energy potential in the European domain with a focus on the Black Sea. Renew. Sustain. Energy Rev. 2018;81(2):1652-1659.
5. Schaeffer R, Szklo AS, Pereira LAF, Moreira CBBS, Pupo NLP, Fleming FP, et al. Energy sector vulnerability to climate change: A review. Energy. 2012;38(1):1-12.
6. Joel N, Jackson N, Simon M. Regional flow duration curve estimation and its application in assessing low flow characteristics for ungauged catchment. A Case Study of Rwegura Catchment-Burundi. Nile Basin Water Sciences & Engineering Journal. 2011;4(1).
7. Bamber P, Guinn A, Gereffi G. Burundi in the energy global value chain: Skills of private sector development. North Carolina, USA: CGGC Duke University; 2014.
8. Riaz V, Kevin L, Andy B, Nhlanhla M, Bruno C. Planning issues for newly industrialized and developing countries (Africa). Eskom, Johannesburg, South Africa: CIGRE WG C1.9; 2013.
9. Bidou JE, Ndayirukiye S, Ndayishimiye JP, Sirven P. Géographie du Burundi (Geography of Burundi). Paris, France: Hatier; 1991.
10. MATTE. National communication strategy on adaptation to climate change and precautionary warning of extreme climate events. Bujumbura, Burundi; 2014.
11. Asfaw A, Simane B, Hassen A, Bantider A. Variability and time series trend analysis of rainfall and temperature in Northcentral Ethiopia: A case study in Woleka sub-basin. Weather and Climate Extremes. 2018;19:29–41.
12. Ioannis Z. Combining multiple imputation with cross-validation for calibration and assessment of cox prognostic survival models. Leiden, Netherlands: Leiden University; 2017.
13. Rasmus EB, Abdelkader M, Kajsa MP. esd: Climate analysis and empirical-statistical downscaling (ESD) package for monthly and daily data; 2015. Available:https://github.com/metno/esd
14. Giorgi F, Jones C, Asrar G. Addressing climate information needs at the regional level: The CORDEX framework. World Meteorol. Org. Bull. 2009;58:175-183.
15. Youm JS, Sall M, Ndiaye A, Kane MM. Analysis of wind data and wind energy potential along the northern coast of Senegal. Rev. Energ. Ren. 2005;8:95-108.
16. Wilkie J, Leithead WE, Anderson C. Modelling of wind turbines by simple models. Wind Engineering. 1990;14(4): 247-274.
17. Kendall MG. Rank correlation methods. Hafner Publishing Co. Ltd.; 1962.
18. Mann HB. Nonparametric tests against trend. Econometrica. 1945;13:245-259.
19. George YL, David WW. An adaptive inverse-distance weighting spatial interpolation technique. Computers & Geosciences. 2008;34(9):1044–1055.
20. Schulzweida U, Kornblueh L. CDO user's guide climate data operators version 1.0.6: Max-Planck-Institute for Meteorology and Ralf Quast Brockmann Consulting; 2006.
21. RCoreTeam R: A language and environment for statistical computing. R Foundation for Statistical Computing Vienna, Austria; 2018.

Available:https://www.R-project.org/
22. Ayodele TR, Jimoh AA, Munda JL, Agee JT. A statistical analysis of wind distribution and wind power potential in the coastal region of South Africa. International Journal of Green Energy. 2013;10(8):814-834.
23. Bilal BO, Ndongo M, Sambou V, Ndiaye PA, Kebe CM. Diurnal characteristics of the wind potential along the North-western coast of Senegal. International Journal of Physical Sciencies. 2011;6(35):7950-7960.
24. Bloom A, Kotroni V, Lagouvardos K. Climate change impact of wind energy availability in the eastern mediterranean using the regional climate model PRECIS. Natural Hazards and Earth System Sciences. 2008;8(6):1249-1257.
25. Choge DK, Maritim JK, Arusei GK, Yegon GK. Small wind turbines: A simulation for optimal selection in uashu-gishu, Kenya. International Journal of Advanced Research. 2013;1(8):508-515.



*Peer-review history:*
*The peer review history for this paper can be accessed here:*
*http://www.sdiarticle3.com/review-history/47337*